Transactions, SMiRT-25
Charlotte, NC, USA, August 4-9, 2019
Division IV

AN OVERVIEW OF HIGH-FREQUENCY GROUND MOTION CHARACTERISTICS OF ROCK SITES IN EASTERN CANADA

Samantha M Palmer[1], Gail M Atkinson[2]

[1] PhD Candidate, University of Western Ontario, London, ON, Canada (spalme22@uwo.ca)
[2] Professor of Earth Sciences, University of Western Ontario, London ON, Canada (gatkins6@uwo.ca)

ABSTRACT

We examine high-frequency ground motion characteristics of rock sites in eastern Canada as expressed by kappa, the parameter that measures high-frequency spectral decay of the Fourier amplitude S-wave acceleration spectrum (Anderson and Hough, 1984). Using 137 records from earthquakes of **M**≥3.5 at distances<150 km, we determine site kappa (κ_0) and apparent attenuation (Q_a) for 9 eastern Canadian seismograph stations sited on rock. Plots of kappa versus epicentral distance produce a linear trend that is attributed to anelastic attenuation (the inverse of the regional Quality factor, Q). We determine κ_0 (the zero-distance intercept of kappa) and the associated Q_a at high frequencies (~21 to 36 Hz) that explains the distance trend. Q_a is the value of Q that results in a flat linear trend of kappa with epicentral distance, and κ_0 is the mean kappa value after correcting spectra for the effects of anelastic attenuation (Q_a). We find that κ_0 values for rock sites range from 0 to 0.01 seconds, with Q_a ranging from 1700 to >6000. We observe that the horizontal components have larger kappa values than the vertical components. Apparent Q values are larger on the vertical component than on the horizontal component, suggesting lower anelastic attenuation at high frequencies.

INTRODUCTION

Nuclear plants are sensitive to high-frequency earthquake ground motions. In eastern North America, most plants were built to an earthquake design spectrum that is robust at lower frequencies but may be deficient at high frequencies for some sites founded on very hard rock – which can effectively transmit high-frequency motions. High-frequency motions from moderate earthquakes can cause exceedance of the design basis earthquake, especially at frequencies greater than 10 Hz, leading to costly outages even if no damage occurred (e.g. Leblanc and Klimkiewicz, 1994).

In eastern Canada there are 5 nuclear power plants, all of which were sited on various types of rock foundations. These sites are in Ontario (at Bruce, Pickering and Darlington), Quebec (Gentilly; note this plant is no longer operating) and New Brunswick (Point Lepreau). Siting on rock minimizes site amplification, which is beneficial at low frequencies (<10 Hz). However, rock also minimizes high-frequency attenuation in the near-surface, which can result in greater motions at high frequencies (>10 Hz) in comparison to soil. The high-frequency characteristics of ground motions and how they depend on rock site conditions is a significant topic for seismic design and safety reviews for nuclear plants. The aim of this work is to characterize high-frequency ground motion parameters on various rock sites in eastern Canada. This will improve our understanding of the amplitudes of ground motions that nuclear plants need to withstand, and their dependence on frequency at various rock sites.

Ground motions (Y) recorded at a site are modelled in the Fourier domain as the multiplication of the source (E), path (P), site (G), and instrument (I) responses, as shown in Equation 1:

$$Y(M_0, R, f) = E(M_0, f)P(R, f)G(f)I(f) \quad (1)$$

Where M_0 is the seismic moment, R is a distance parameter such as epicentral distance, and f is frequency (Boore, 2003). This study aims to understand the influence of rock site conditions on ground motions at high frequencies. We therefore need to separate the effects of the site from those of source and path. Path effects are described by the combination of geometric spreading, which is frequency-independent, and anelastic attenuation, which is an increasing function of frequency. The effects are described in the path component of ground motion models as:

$$P(R, f) = Z(R)e^{-\frac{\pi f R}{Q(f)\beta}} \quad (2)$$

Where β is the average crustal shear wave velocity, and $Z(R)$represent geometrical spreading (Boore, 2003). In Equation (2), we have represented anelastic attenuation using the regional Quality factor, Q, to which it is inversely proportional. Atkinson and Mereu (1992) describe southeastern Canada attenuation as Q=$670f^{0.33}$. Mereu et al (2013) determined a similar relation for Q in eastern Canada, $526f^{0.51}$, applicable for frequencies of 1Hz to 43 Hz.

The site component of ground motions (G) is a combination of amplification and attenuation effects, both of which are frequency-dependent. The attenuation effects can be described by a steady linear decay of the log of spectral amplitude with increasing frequency. The slope of the decay trend is characterized by the parameter kappa (κ), originally introduced by Anderson and Hough (1984:

$$A(f) = A_0 e^{-\pi\kappa f} \quad (3)$$

Where A is the Fourier amplitude of acceleration for the S-wave window, A_0 is the amplitude, and κ is the spectral decay parameter. κ can be considered to comprise several components (Ktenidou et al., 2014):

$$\kappa = \kappa_0 + \kappa_s + \tilde{\kappa}(R_e) \quad (5)$$

Including a site-specific portion (κ_0), a source-dependent portion (κ_S) and a distance dependence, which is related to the anelastic attenuation ($\tilde{\kappa}(R_e)$).

Atkinson (1996) examined kappa values in Ontario, Quebec and New Brunswick and determined that there was no resolved kappa effect on vertical-component spectra for hard-rock sites in most parts of eastern Canada. She suggested an upper bound kappa value of 0.004 s for hard-rock sites. However, higher kappa values, of 0.02 to 0.04 s, were found for sites within the fractured rocks of the Sudbury and Charlevoix meteor impact craters. Campbell et al. (2014) utilized earthquake data from Central Eastern North America, which included earthquakes from eastern Canada, to determine an overall regional kappa value of 0.006 s. Ktenidou et al. (2016) determined a kappa value of 0.007 s for rock sites using the NGA-East Database, which includes data from across central and eastern North America. Thus, previous studies suggest a range of possible kappa values for rock sites in the east, and the potential for variability due to rock conditions such as degree of deep-seated fracturing. To understand the variability of kappa in eastern Canada we compile a comprehensive database of earthquake ground motions on rock sites and use that data to resolve high-frequency site effects.

METHODOLOGY AND DATABASE

Dataset

Ground motions in eastern Canada are continuously recorded on dozens of broadband seismographic stations by the Canadian National Seismographic Network (CNSN) and the Southern Ontario Seismographic Network (SOSN). Broadband seismographic stations in eastern Canada measure ground motion in either one direction (vertical) or 3 directions (vertical, East-West, North-South). The horizontal-component ground motion is often represented by the geometric mean of the East-West and North-South components. The broadband seismographic stations utilized in this study continuously sample velocity at 100 samples/s. The 9 seismic stations selected for this study include those near Charlevoix, Quebec: A11, A16, A21, A54, A61, A64, DAQ and a few at the mouth of the St. Lawrence River: GSQ and CNQ. We utilize earthquakes recorded within 150 km of these stations that have a moment magnitude (**M**) greater than 3.5, recorded from August 1989 to May 2018, and having at least 5 observations from which to measure kappa. Figure 1 shows selected earthquakes and the 9 seismic stations of this study.

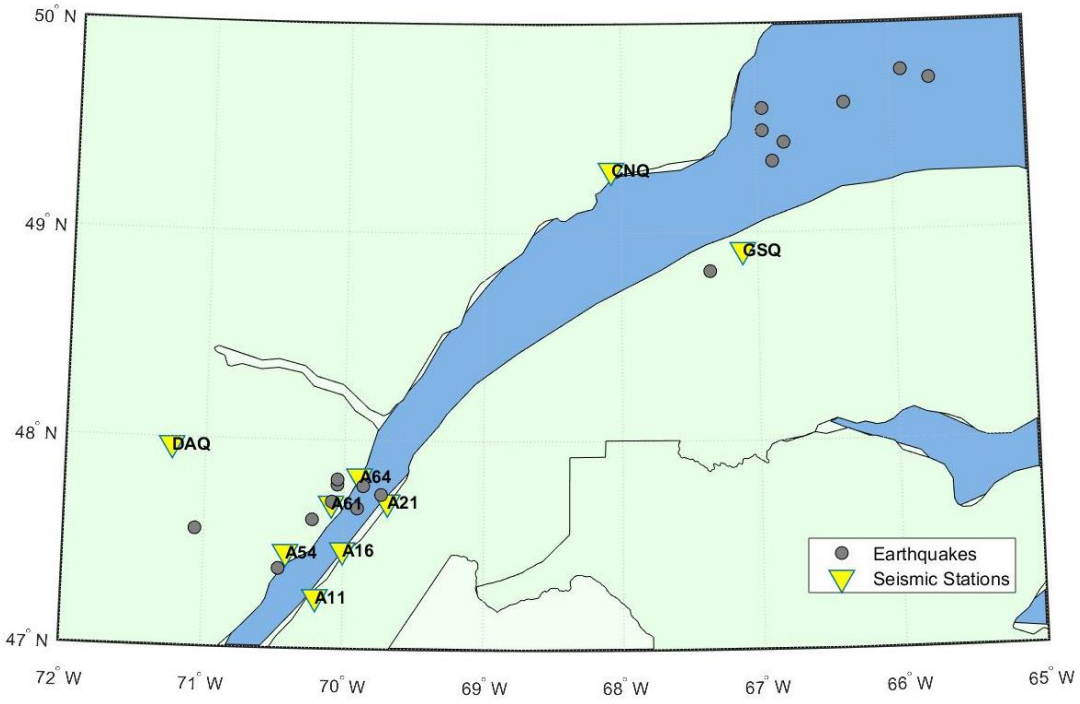

*Figure 1: **M** >3.5 earthquakes (grey circles) for the 9 selected seismic stations (yellow inverted triangles) utilized to measure kappa and apparent attenuation in Eastern Canada.*

The Geological Survey of Canada (GSC; Earthquakes Canada) reports earthquake magnitudes on several scales, including the local magnitude and Nuttli magnitude scales. To better reflect the actual size of an earthquake and provide one consistent magnitude type, we convert all magnitudes to moment magnitude (**M**) using the conversions of the Fereidoni et al. (2012) Composite Canadian Seismicity Catalogue. A total of 137 velocity time series from 9 stations and 21 earthquakes make up the database of ground motions used to determine κ and Q_a; their distribution in magnitude and distance is shown in Figure 2. All seismic stations are either directly in contact with rock or sit on a concrete platform in contact with the rock. This was confirmed by a site visit to each station. Estimated bedrock velocities range from 1000 m/s to 3200 m/s at the 9 sites of this study (Ladak, personal communication).

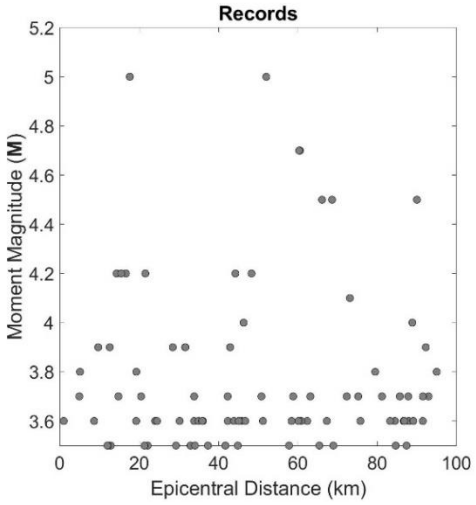

*Figure 2: Distribution of records for 21 earthquakes on 9 stations by moment magnitude (**M**) and epicentral distance.*

Data Processing

We calculated the Fourier amplitude spectrum of the S-wave portion of the signals as follows. Velocity time series and instrument response files, in SEED format, were retrieved from the Earthquakes Canada waveform AutoDRM email service (AutoDRM@seismo.NRCan.gc.ca). We retrieved 360 seconds of signal, starting 70 seconds prior to the earthquake start time, for each record. The utility program rdSEED (from www.iris.org) was used to convert the files into SAC files (where SAC, Seismic Analysis Code, is a seismological processing software available through IRIS (Goldstein and Snoke, 2005; Goldstein et al. 2003)) which contain the time series, and RESP files which contain the instrument response data. We used standard SAC processes to process the time series by:

- removing the mean, detrending, and tapering the entire time series,
- removing the instrument response from the entire time series in the Fourier domain (note the valid range of data is from 0.3 to 40 Hz after applying this correction),
- selecting the S-wave and P-wave arrivals,
- cutting the full instrument-corrected time series signal 0.5 seconds prior to the S-wave arrival and 14.5 seconds after, to obtain a 15 second S-window,
- cutting the full instrument-corrected time series signal 20 seconds prior to the P-wave arrival and 5 seconds prior to the P-wave arrival to obtain a 15 second noise window,
- Applying the FFT function,
- Differentiating, using SAC's mulomega function, to obtain the Fourier amplitude spectrum of acceleration.

Sample processed time series and Fourier amplitude spectra are shown in Figure 3 at two different stations for the same earthquake. An S-wave and noise time series are produced to be able to determine the frequency range having adequate signal to noise ratio (>3), over which kappa can be measured. We generated instrument response spectra using SAC's standard process, to determine the range where the instrument response is flat. Additionally, we generated smoothed Fourier amplitude spectra using the Konno Ohmachi smoothing method with a b value of 20. We computed the horizontal to vertical spectral ratio for each station having both vertical and horizontal records. The resultant database produced after

processing consists of the time series for both S-wave and noise, the corrected Fourier amplitude spectra for both S-wave and noise, the instrument response spectra for the record, smoothed Fourier amplitude spectra for both S-wave and noise, and the horizontal to vertical spectral ratios for the S-wave window. The example spectra plotted on Figure 3 show the classic shape expected for a simple earthquake source model (Boore, 2003), in which the acceleration rises as the square of frequency to a corner frequency, which depends on earthquake magnitude; larger earthquakes are richer in low-frequency energy, and thus have lower corner frequencies, in comparison to small earthquakes. Above the corner frequency, the acceleration spectrum is approximately constant in amplitude, except for the effects of anelastic attenuation (path) and kappa (site), which cause a gradual decay trend with increasing frequency.

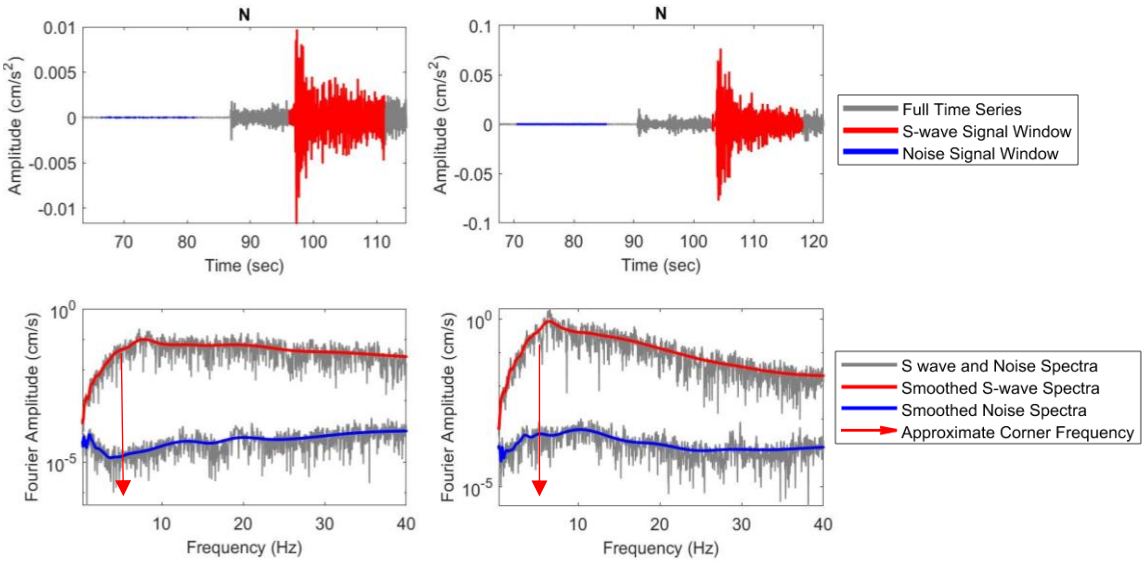

Figure 3: Example of windowed time series and Fourier amplitude spectra for the N-S component for the earthquake recorded on 2000/07/12 at 15:01:49 on two stations: A16 (left) and A21 (right). S-window is shown in red in the time series plot (top). Fourier amplitude spectrum of the signal before smoothing (grey) and after smoothing (red; Konno Ohmachi b = 20) (bottom). Red arrows mark the approximate corner frequency (~5 Hz) of the spectra. The corresponding spectra for the noise window are also shown (in grey and blue).

To determine κ and Q_a we first determine the frequency range over which the spectra computed are valid. By valid we mean that the spectra are not contaminated by a non-flat instrument response or by noise. The instrument response is generally flat in our examined frequency range from 0.3 Hz to 40 Hz; we check to ensure that for each record the instrument response amplitude is not less than half its maximum value. We require that the signal to noise ratio, obtained by dividing the amplitude of S-wave spectrum squared by the amplitude of the noise spectrum squared, be >3 over the frequency range considered.

Compute Kappa

We determine kappa utilizing a variant of Anderson and Hough's (1984) classical method, in which we consider a fixed frequency range. To isolate high-frequency site effects from source effects, we wish to ensure that we are measuring kappa at frequencies greater than 1.5 times the earthquake's corner frequency (see Fig. 3). The corner frequency for each record was first estimated as the lowest frequency at which ½ of the maximum amplitude of the Fourier amplitude spectra is attained (Boore, 2003). Figure 4 is a histogram of corner frequencies for all records in this study. Note that 90 % of the records have an estimated

corner frequency below 14 Hz. We therefore chose a minimum frequency of 21 Hz (=1.5 * 14 Hz) for kappa measurements, to ensure we are well above the corner frequencies of the study events. To choose the maximum frequency, we note that most records had good signal-to-noise ratio up to 40 Hz. We selected a maximum frequency of 36 Hz; choosing a high-frequency limit slightly less than the maximum frequency allows evaluation of the sensitivity of kappa estimates to the selected frequency range, as will be discussed later. Therefore, we measure κ from 21 Hz to 36 Hz on each record having a lowest useable frequency <21 Hz and a highest useable frequency >36 Hz. The lowest useable frequency (LUF), as defined by Ktenidou et al. (2016), is defined as the maximum value of: the lowest resolvable frequency of the spectrum (<<1 Hz in this study); the low-frequency limit imposed by the instrument response (<< 1 Hz in this study); the lowest frequency imposed by the signal to noise criterion; and the half-maximum corner frequency*1.5. The highest useable frequency (HUF), also defined by Ktenidou et al. (2016), is the minimum value of: the upper frequency imposed by the instrument response; the upper frequency imposed by the signal to noise criterion. Records that have a LUF >21 Hz or a HUF <36 Hz are not included in the computation of κ, allowing the use of a single frequency range (21 to 36 Hz) for consistency of kappa determinations.

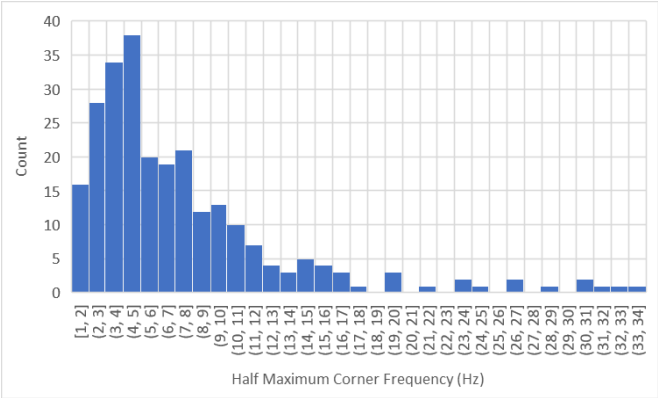

Figure 4: Histogram depicting the half maximum estimate corner frequency for the 137 records of this study.

To ensure that the kappa measurements are not overly sensitive to the selected limits of the frequency range considered, we follow the approach of Perron et al. (2017) in estimating its uncertainty. In this approach, f_1 (the lower bound from which to measure κ) and f_2 (the upper bound from which to measure κ) are varied by an increment of δf; κ is determined by applying a linear regression to Eqn. (3) over all frequency ranges given by $f_1 \pm \varepsilon_1 \delta f$ and $f_2 \pm \varepsilon_2 \delta f$ where ε_1 and ε_2 are random numbers between 0 and 1. We use a simplified version of this method in which f_1, f_2, ε_1, ε_2 and δf are all given fixed values. In this study, we vary the upper and lower frequency limits by the increment δf = 2 Hz, which was selected to avoid encroaching on the corner frequency of most records and fix ε_1 and ε_2 at 1. We measure kappa over all combinations of the frequency ranges given by $f_1 \pm \delta f$ to $f_2 \pm \delta f$. Using the linear regression slope of the unsmoothed spectrum, fit to Eqn (3), we determine κ by dividing by -π. Figure 5 shows a sample Fourier amplitude spectrum and the measurement process for κ. From the 9 frequency ranges over which we measure κ, we determine the mean and median κ. The mean and median κ values are similar, with the median value lying within the standard error of the mean. In measuring κ there are two significant sources of uncertainty: (i) the choice of frequency range leads to variability in the computed values; and (ii) amplitude variability of the spectra leads to measurement uncertainty on the slope (for a single frequency range). We report the error as the maximum value of: (i) the standard error of the 9 measured κ values (i.e. from $f_1 \pm \delta f$ to $f_2 \pm \delta f$); and (ii) the maximum standard error of the slope as obtained from the 9 linear regressions. The second error value is, in general, within the standard error of the 9 measured kappa values over the various frequency ranges. Therefore, the amplitude variability of the spectrum contributes less to measurement uncertainty than does the frequency range over which κ is measured.

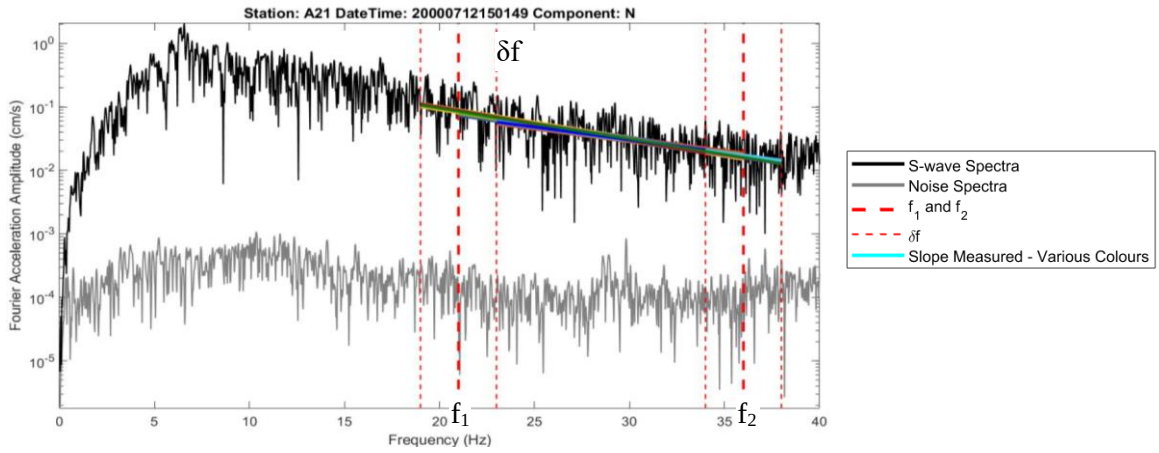

Figure 5: Example of measuring kappa and its associated variability for earthquake 2000/07/12 15:01:49 recorded on station A21. The thick vertical red dashed lines represent f_1, the lower bound for the κ measurement, and f_2, the upper bound for the κ measurement. The thin vertical red dashed lines show the frequency increment applied to evaluate variability, δf, (i.e. ±2 Hz about f_1 and f_2). The S-wave Fourier amplitude acceleration spectrum is shown in black and the noise Fourier amplitude acceleration spectrum is shown in grey. Solid lines show the 9 slope determinations.

Compute Apparent Attenuation

The kappa values measured from each record contain contributions from both path and site effects. To isolate these contributions, we plot the determined values of κ at each station as a function of distance from the earthquake source. The site component of kappa, κ_0, is its observed value at close distances, whilst the increase in measured kappa with distance is driven by the contributions of anelastic attenuation. The effects of anelastic attenuation on the spectrum are to reduce amplitudes according to $e^{-\pi f R/Q\beta}$(Eqn 2). If we know the value of Q over the frequency range of interest (21 – 36 Hz), then we can correct for these effects to infer κ_0. Alternatively, we can use the increase in measured kappa with distance to infer Q in the area surrounding each station. To do this, we assume that Q is approximately constant over the frequency range from 21-36 Hz. Based on previous studies (e.g. Mereu et al., 2013), we assume a Q value, in this frequency range, between 1000 to 6000. We assume β = 3.7 km/s (mid-crustal velocity). We use a grid search approach to find the apparent value of Q for each station, searching over the range from 1000 to 6000 in increments of 100. For each value, we apply the corresponding attenuation correction to the spectra before computing kappa. The Q value that produces a zero-distance trend to kappa is taken as the apparent attenuation (Q_a) in the region surrounding that station. (Note: In the case where multiple trial Q values result in a 0-distance trend we report the middle Q value, to the nearest 100. If there are an even number of Q values that produce a distance-trend of 0, the lower middle value is selected.) The value of κ_0 at each station is then taken as the average of the attenuation-corrected kappa values (which is also the intercept of the trend-corrected kappa values versus distance). In the case where Q_a is >6000, the reported κ_0 is defined as the mean κ at epicentral distances < 100 km.

RESULTS AND DISCUSSION

Figure 6 shows the relationship between κ and epicentral distance before (circles) and after (triangles) attenuation corrections, for four of nine stations. In general, κ values are relatively insensitive to distance within 50 to 100 km, which is as expected based on the exponential effects of distance on anelastic

attenuation, and in agreement with the findings of Ktenidou et al. (2016). As a result, κ_0 could be determined either by correcting for attenuation and obtaining the value at zero epicentral distance, or by simply averaging the measured κ values for stations within 50 to 100 km. Due to the paucity of earthquakes recorded at close distances, particularly on some stations (DAQ, GSQ, and CNQ), we prefer the approach of estimating κ_0 based on the attenuation-corrected values of κ. Table 2 provides the values of κ_0 and Q_a determined for each station having at least five observations of events of **M**≥3.5 within 150 km.

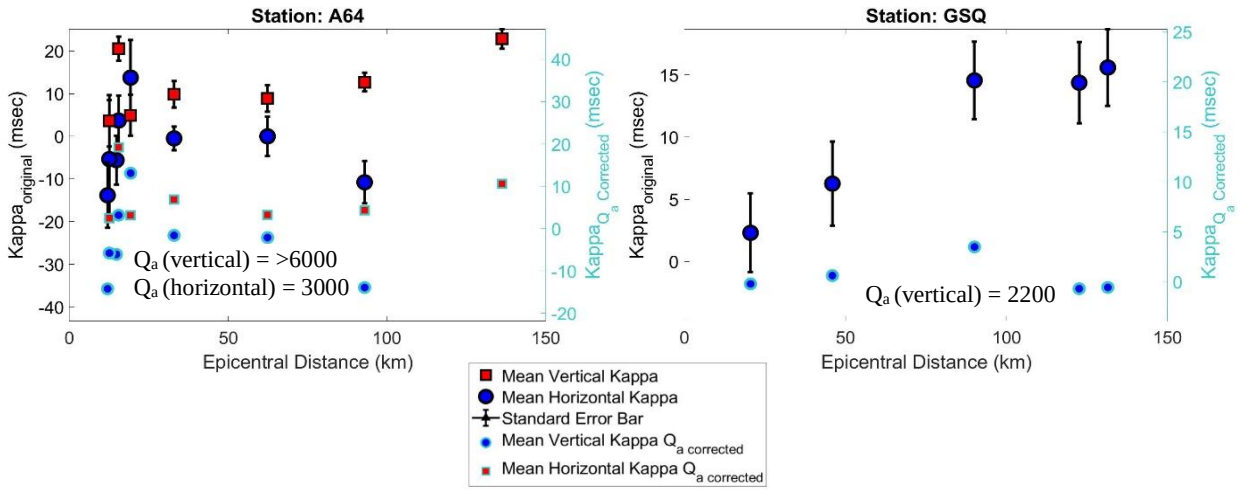

Figure 6: values at stations A64, and GSQ. Horizontal component (red squares black outline) κ and vertical component (blue circles black outline) κ values show κ measured from spectra prior to corrections for attenuation. Standard error is represented by error bars (black). Q-corrected κ values are shown as red cyan outlined squares (horizontal component) or blue cyan outlines circles (vertical component); Values of Q_a to obtain zero distance trend are given.

The values of κ_0 and Q_a vary considerably from site to site, but the values of κ measured on the horizontal component tend to be consistently larger than those on the vertical component, whilst the apparent Q values are larger on the vertical than on the horizontal. Both observations are consistent with lesser attenuation of high-frequency energy on the vertical component.

To evaluate whether the values of κ might be significantly influenced by near-surface site amplification effects, we examine horizontal to vertical spectral ratios (HVSR). The HVSR is a well-known proxy for site response (e.g. Nakamura, 1989; Lermo and Chavez-Garcia, 1993). The idea is that site amplification effects are stronger on the horizontal than on the vertical component, and thus site amplification can be measured, approximately, by the HVSR. On stations with both horizontal and vertical component records we can measure the HVSR directly from the records compiled in this study. At stations where there are only vertical component records, we rely on the measurements of Ladak et al. (2019, submitted paper) who used active and passive methods to determine the HVSR at seismographic stations in eastern Canada, including those of this study. Based on the earthquake records, stations A11, A16, A21, A54, and A64 are characterized by relatively flat HVSR with amplitudes <2 at all frequencies and are thus believed to be relatively free of significant site amplifications. Station A61 has a frequency peak near 20 Hz, indicating a possible bias in the measured values of κ. Ladak et al. (2019) report that CNQ has a peak frequency near 5 Hz, which should not affect the κ measurement between 21 to 36 Hz. DAQ has a HVSR that is relatively flat from 2 Hz to 40 Hz, but has a high amplitude (Ladak et al., 2019). GSQ has a flat HVSR with low amplitude (Ladak et al., 2019). Thus, based on the HVSR the kappa values at all stations except A61 are likely to be relatively unaffected by site amplification effects.

In Table 1, it is interesting to note that in some cases we report negative values for κ_0, implying a slight positive trend in amplitudes with increasing frequency after correction for attenuation effects. (Note: negative values are also measured for some records before attenuation corrections.) This is not considered meaningful in view of the uncertainty in the attenuation corrections; thus, negative κ should be considered as near-zero κ_0. The attenuation of the spectra at high frequencies is an area for further investigation. The application of both kappa and anelastic attenuation corrections is consistent with the way these parameters are used in the development of ground motion models (e.g. Boore, 2003). The values that we infer for attenuation, based on the limited records in this study, are consistent with expectations based on more comprehensive attenuation studies. For example, Atkinson and Mereu (1992) and Mereu et al. (2013) model attenuation in eastern Canada over a wide range of distances and frequencies. They infer that at high frequencies (21 to 36 Hz), Q is in the range from 1800 to 3300. Our results suggest an apparent Q between 1700 and >6000, which is generally consistent with this range. The high values of Q_a obtained for the vertical component on a few stations suggests that high-frequency attenuation is often minimal for rock sites for distances within 100 km.

Table 1: Values of κ_0 and Q_a. Note: stations with Q_a denoted >6000 κ_0 values are computed using the average of κ values with epicentral distances less than 100km. Negative values of κ_0 imply increasing spectral amplitudes with frequency, after Q corrections, and should be considered equivalent to κ_0 ~0.

Station	Horizontal κ_0 (msec)	Horizontal Q_a	Vertical κ_0 (msec)	Vertical Q_a
A11	4±7	1700	-11± 4	4100
A16	5±4	4800	-8±7	>6000
A21	16±7	1700	11±5	5700
A54	-4±2	2300	2±2	>6000
A61	45±6	2900	2±4	>6000
A64	7±4	3000	-2±3	>6000
CNQ	N/A	N/A	-10±23	1900
DAQ	N/A	N/A	-5±4	1900
GSQ	N/A	N/A	1±2	2200

CONCLUSION

Overall, we find that site-specific kappa values, κ_0, in eastern Canada range from ~ 0 to 0.01 seconds. The wide variability of κ_0 from site to site suggests that κ_0 may be a site-specific parameter rather than a regional parameter. Therefore, site-specific studies based on earthquake recordings are required for robust determination of high frequency site effects for critical infrastructure. We observe that kappa is greater on the horizontal component in comparison to the vertical component, as are the effects of anelastic attenuation. Future work will expand the database for kappa evaluations to include smaller events and will study the relationship between measured kappa values and rock properties.

ACKNOWLEDGEMENTS

We thank Earthquakes Canada for their database and access to the waveforms. We would also like to thank Dr. Sheri Molnar, Sameer Ladak, Dr. Hadi Ghofrani, and Joanna Holmgren for insightful discussion. Funding for this project was provided by the Canadian Nuclear Safety Commission.

REFERENCES

Atkinson, G.M., and Mereu, R.F. (1992) "The Shape of Ground Motion Attenuation Curves in Southeastern Canada," *Bulletin of the Seismological Society of America,* 82(5) 2014 – 2031.

Atkinson, G.M. (1996) "The High-Frequency Shape of the Source Spectrum for Earthquakes in Eastern and Western Canada," *Bulletin of the Seismological Society of America,* 86(1A) 106 – 112.

Anderson, J. and Hough, S. (1984) *"A Model for the Shape of the Fourier Amplitude Spectrum of Acceleration at High Frequencies," Bulletin Seismological Society of America*, 74(5) 1969 – 1993.

Anderson, J.G. and Humphrey, J.R. (1991) *"A Least Squares Method for Objective Determination of Earthquake Source Parameters," Seismological Research Letters*, 62(3-4) 201 – 209.

Boore, D.M. (2003) "Simulation of Ground Motion Using the Stochastic Method," *Pure and Applied Geophysics*, 160 635-676.

Campbell, K.W, Hashash, Y. M.A., Kim, B., Kottke, A.R., Rathje, E.M., Silva, W.J., and Stewart, J.P. (2014) "Reference-Rock Site Conditions for Central and Eastern North America: Part II – Attenuation (Kappa) Definition." PEER Report 2014/12.

Fereidoni, A., Atkinson, G.M., Macias, M., and Goda, K. (2012) "CCSC: A Composite Seismicity Catalog for Earthquake Hazard Assessment in Major Canadian Cities," *Seismological Research Letters*, 83(1) 179 – 189.

Goldstein, P., and Snoke, A. (2005), "SAC Availability for the IRIS Community," Incorporated Institutions for Seismology Data Management Center Electronic Newsletter.

Goldstein, P., Dodge, D., Firpo, M., and Minner, L. (2003) "SAC2000: Signal processing and analysis tools for seismologists and engineers", *The IASPEI International Handbook of Earthquake and Engineering Seismology*, Academic Press, London

Hanks, T.C. (1982) *"fmax," Bulletin Seismological Society of America*, 72(6) 1867 – 1879.

Ktenidou, O., Cotton, F. Abrahamson, N. A., and Anderson, J. G. (2014) *"Taxonomy of κ: A Review of Definitions and Estimation Approached Targeted to Applications," Seismological Research Letters,* 85(1) 135 – 146.

Ktenidou, O.J., Abrahamson, N.A., Darragh, R.B., and Silva, W.J. (2016) "A Methodology for the Estimation of Kappa (κ) from Large Datasets: Example Application to Rock Sites in the NGA-East Database and Implications on Design Motions" PEER Report No. 2016/01.

Ladak, S., Molnar, S., Palmer, S.M., and Atkinson, G.M. (2019) "Application of Active and Passive Seismic Methods for Determining the Shear Wave Velocity Profile at Hard Rock Site in Eastern Canada," *12th Canadian Conference on Earthquake Engineering,* Quebec City, Quebec, submitted publication.

Leblanc, G.A., and Klimkiewicz, G.C. (1994) "Seismological Issues: History and Examples of Earthquake Hazard Assessment for Canadian Nuclear Generating Stations," Geological Survey of Canada Open File 2929.

Lermo, J. and Chávez-García, F.J. (1993) "Site Effect Evaluation Using Spectral Ratios with Only One Station," *Bulletin of Seismological Society of America,* 83(5) 1574-1594.

Mereu, R. F., Diveva, S., and Atkinson, G.M. (2013) "The Application of Velocity Spectral Stacking to Extract Information on Source and Path Effects for Small-to-Moderate Earthquakes in Southern Ontario with Evidence for Constant-Width Faulting," *Seismological Research Letter,* 84(5) 899 – 916.

Nakamura, Y. (1989) "A Method for Dynamic Characteristics Estimation of Subsurface Using Microtremor on the Ground Surface," *Reailway Technical Research Institute, Quarterly Reports,* 30(1) 25-33.

Perron, V., Hollender, F., Bard, P. Gélis, C., Guyonnet-Benaize, C., Hernandez, B., and Ktenidou, O. (2017) "Robustness of Kappa (κ) Measurement in Low-to_moderate Seismicity Areas: Insight from a Site-Specific Study in Provence, France," *Bulletin Seismological Society of America*, 107(5) 2272 – 2292.